Modelling for Coat Thickness Measurements of Thin Printed Films

Jacqueline Stamm, Dominik Daume, Maximilian Oschmann, Hans-Martin Sauer and Edgar Dörsam

Technische Universität Darmstadt, Institute of Printing Science and Technology, Germany

ISCST-20180918PM-A-PD2

Presented at the 19th International Coating Science and Technology Symposium,
September 16-19, 2018, Long Beach, CA, USA†.

Motivation

Creating homogeneous films is extremely important in the field of printed, organic electronics, as they influence the performance of the printed elements. There are examples in flexo printing SMOLEDs (small molecule organic light-emitting diodes) (Raupp, 2017) and gravure printing OLEDs (Bornemann, 2014). The phenomena leading to these unwanted inhomogeneities are investigated, too, for example the ink splitting while flexo printing (Griesheimer 2014).

The main problem while printing is the development of inhomogeneous films during the printing process aided by hydrodynamic instabilities and drying phenomena (Hernandez-Sosa, 2013; Toolan, 2015).

To characterize the homogeneity of printed films a method is needed for analyzing the topography of the final film thickness. Furthermore, if the film inhomogeneities are to be linked to the printing and drying process the method has to track the film development time and space-resolved.

The goal is to develop an optical measurement procedure and analysis method for tracking the film thickness evolution of large-area drying thin films over time using the example of gravure printing. The method will evaluate RGB-values of the acquired pictures during the drying process and rely on the correlation between interference induced intensity changes and the change in film thickness.

State of the art

There are several approaches for connecting the interference intensities at solid thin films to their area-resolved thickness (Bornemann, 2014; Birnie, 2004; Kitagawa, 2013; Parthasarathy, 1987). After initial tests two were proven as most promising and will be introduced. There is also a way of tracing the thickness development of a small point over time (Toolan, 2015; Ebbens, 2011), but no literature connecting both was found.

Bornemann's method uses white light as illumination and calculate theoretically the expected interference colors resulting from different film thicknesses as RGB-values. But these theoretical values will never match the experimental data, because of unaccounted optical effects that result in unknown multiplicative constants. To avoid the need for calculating these constants contrast value triplets $c_k = (c_R, c_G, c_B)$ are calculated that connect the intensity values of a certain thickness A_k with the intensity values of the reference with zero thickness $A_{k,ref}$ by:

$$c_k = \frac{A_k - A_{k,ref}}{A_k + A_{k,ref}} . \quad (1)$$

The experimental values are converted in the same way. If both image and reference image were acquired under the same conditions the unknown constants are equal and cancel.

The other method is given by fitting a cosine waveform to the intensities over film thickness of each RGB-value acquired from a known data base, like Kitagawa. The observed intensity $g(i,\lambda)$ at the place i and illuminated with wavelength λ can be expressed as:

$$g(i,\lambda) = a(\lambda)[1 + b(\lambda)\cos\{\Phi(i,\lambda)\}] \quad (2)$$

† Unpublished. ISCST shall not be responsible for statements or opinions contained in papers or printed in its publications.

with the phase difference Φ and the waveform parameters *a(λ)* and *b(λ)* as fit parameters, which need a good starting guess. In contrast to other fitting methods red, green and blue illuminations are used consecutively. The wavelengths of the illumination have small band-widths and are chosen to match the filter functions of the camera, leading to a greater spatial coherence l_t, which is essential for stable interference.

$$l_t \cong \frac{\lambda^2}{\Delta\lambda} \tag{3}$$

Toolan's and Ebben's methods look at the whole drying process dependent on the time. They illuminate the drying film with a green small band-width LED. As time goes by the film dries and becomes thinner, making the interference pattern go through maxima and minima. The positions of the maxima in time are plotted, knowing the theoretical difference in thickness *d* between two maxima, which only depend on the refractive index *n* and the illumination wavelength *λ*:

$$d_2 - d_1 = \frac{2\lambda}{2n} - \frac{\lambda}{2n} = \frac{\lambda}{2n} \tag{4}$$

Also, the final thickness has to be known. Either the whole film evaporates leaving a zero thickness in the end or the it has to be determined elsewise. Both methods focus on observing the evolution of micro structure, especially phase separation on a small field of view. It is assumed that the final thickness will be close to homogeneous and a mean thickness determination as obtained by AFM scratch testing and ellipsometry is sufficient.

The ideal film thickness tracking method for larger areas would use this backtracking method, but with an area resolved final thickness map as start parameter. This final thickness map is generated by one of the solid film methods. We have tested the accuracies of these methods and created a new model and setup, which unite all advantages. The use of contrast values by Bornemann is combined with the three wavelengths illumination by Kitagawa to yield an easier, faster and more accurate algorithm.

Developed Model

The new model consists of two parts. The first part, called spatial backtracking, illuminates the drying sample with a small band-width LED and captures the occurring interference in a series of pictures. Each pixel intensity goes through minima and maxima given by equation (4), when evaluating the best fitting RGB-channel for the chosen LED peak wavelength (λ_k). The final thickness of each pixel, which is needed as start parameter, is then determined by One-Lambda. Without rearranging the setup three final pictures are taken with different illumination. Again, only the channel-value closest to λ_k is needed. This procedure has three advantages over Bornemann's original white light illumination. Firstly, the coherence of a small band-width spectrum is greater than that of broad white light. Secondly, the chromaticity calculation needed for generating the theoretical RGB-values (A_k) simplifies from a sum over the whole spectrum to one multiplication:

$$A_k = \sum_{\lambda=400nm}^{700nm} I(\lambda)R(d,\lambda)F^k(\lambda) \;\rightarrow\; A_k = I(\lambda_k)R(d,\lambda_k)F^k(\lambda_k)\,. \tag{5}$$

With *I(λ)* the light intensity for the given wavelength *λ*, *R(d,λ)* the sample reflectance, dependent also on the thickness *d* and $F^k(\lambda)$ the camera's R, G and B filter functions. Thirdly, this simplification makes the light intensity and filter functions multiplicative constants, that cancel when building contrast values as in equation (1). Therefore, the sample reflectance is the only needed parameter when calculating theoretical contrast values. The reflectance is calculated by modeling a stack of thin films using Abeles matrix notation and taking into account backside reflection at the substrate as described in Bornemann's paper. A look-up table is constructed containing the theoretical contrast triplets for different film thicknesses. Each captured pixel is converted into an experimental contrast triplet and matched to the theoretical ones by minimizing the distance in contrast space.

Experimental Setup

The setup achieves orthogonal sample illumination with 4 separately selectable LEDs and orthogonal data capture with a Canon 5D Mark II at the same time by incorporating a beam splitter at a 45° angle. The LED light path is parallelized by a telecentric, which achieves an experimentally determined opening angle of $(0.2247 \pm 0.0008)°$ and a homogeneous luminous field, with a standard deviation from the mean intensity of 3% at most. The used lens has a focal length of $f = 100mm$ and each picture shows a luminous circle with a diameter, which is proportional to the used aperture ratio.

The four LEDs with colors red, green, blue and white are characterized using a spectrometer. The peak positions and widths of the three small band-widths illuminations are obtained from a two term Gaussian fit to the recorded data and shown in Table 1.

Table 1: Characterization of the three LEDs. Peak position and width are taken from a two term Gaussian fit to the recorded spectra. The coherence length is calculated from them using equation (3).

Color	Peak position in nm	Width in nm	Coherence length in nm
red	635	18	22401
green	520	31	8723
blue	471	26	8532

The used samples consist of a gravure printed layer of 3% Polymethyl methacrylate (PMMA) in O-Xylene on a silicon wafer. They were printed with the Superproofer at the Institute for Printing Science and Technology, with a velocity of $3m/s$. The refractive indicex of PMMA was measured using a refractometer and yielded a constant mean refractive index of $1{,}504 \pm 0{,}001$ for all illumiantions.

The pictures of the sample right after printing are taken at maximum speed (first 15 at 4fps, then 0.85fps) in the Canon raw format .CR2 and converted to a grey scale sensor image in .TIFF format using the program dcraw by Dave Coffin. These can be processed by Matlab to extract the undemosaiced pixel information of the individual channels. The channel is chosen according to the illumination: R for red, G for green and B for blue illumination. The final thickness and reference pictures in red, green and blue, as well as the refractive index of the printed material, are converted into a final thickness map by OneLambda. The final thicknesses of each pixel and their intensity change during the drying process give thickness maps for each time step, calculated by Spatial Backtracking.

Results and Discussion

The best results were obtained with PMMA and red illumination. The interference patterns were more distinguished when compared to green and blue illumination, because of the bigger coherence length (see Table 1). The thickness evolution of one pixel is shown in Figure 1 and illustrates the backtracking method. The algorithm recognizes the drying point (red cross) and all maxima (blue crosses) correctly and calculates the thickness change. But the data points have too big time intervals to be sure that the marked maxima lie at the right position and that none have been missed.

After combining the results for each pixel, one can analyze the mean thickness evolution of the whole sample or the thickness maps at different times. The mean thickness is shown in Figure 2 with the central line. Its course shows two linear sections with different drying velocities. The first 9 seconds the film thins with $131 \pm 15\ nm/s$, after that with $45 \pm 5\ nm/s$ until reaching its final dry state. The upper and lower limits of the film thickness are plotted in black. The vertical grey lines show at which time steps pictures for the evaluation were taken.

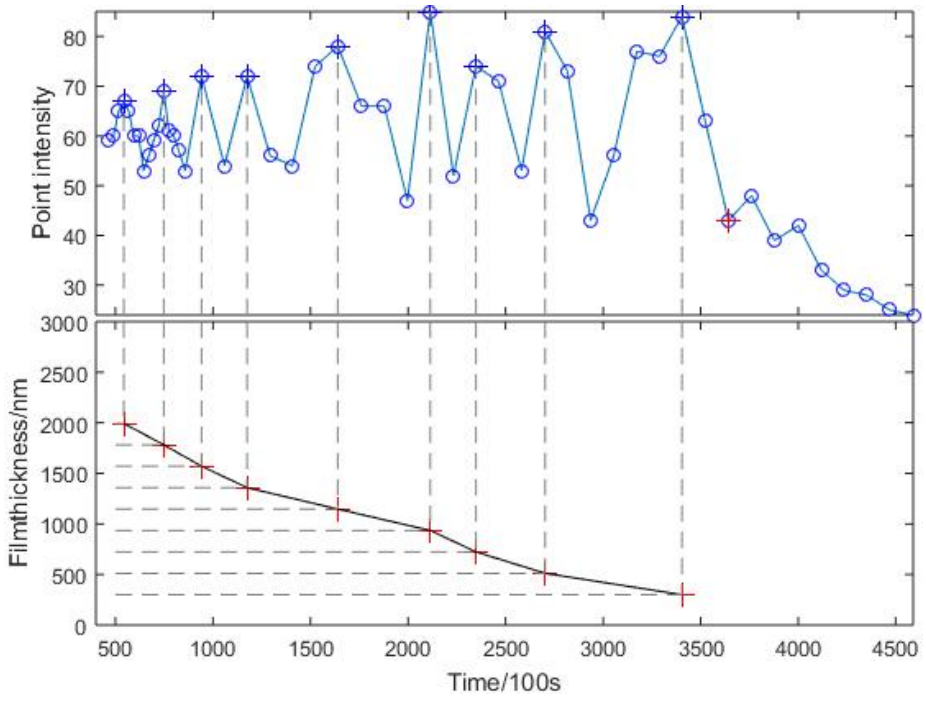

Figure 1: The intensity change of one pixel over time and the corresponding film thickness as calculated by Spatial Backtracking of a PMMA film on silicon and illuminated with the red LED.

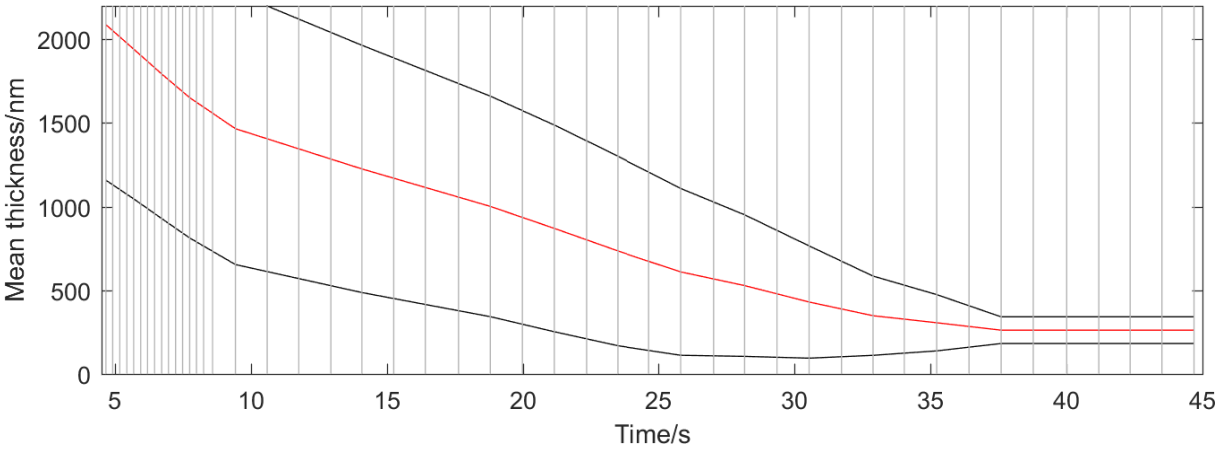

Figure 2: The mean thickness evolution of a PMMA film on silicon and illuminated with the red LED. The mean thickness is shown in red, while the two black lines mark the upper and lower limits calculated by the standard derivative. The vertical lines mark the time steps, when a picture was taken.

Noticeably, the faster drying time overlaps completely with the faster capture time of the camera and raises the question if the capture speed influences the measurements. Probably the slower capture velocity allows interference maxima to pass by without being captured, which was already suggested while analyzing Figure 1. If this were true, all calculated thicknesses would be incorrect by a growing offset towards the initial wet state.

In summary a working set up and algorithm for tracking the thickness development of drying films was introduced and its functionality and results shown on the example of a gravure printed thin film of PMMA on silicon. The weakest point was found to be the capture speed of the used camera. Further experiments with a faster camera could show if the drying velocity actually consists of two linear slopes.

Literatur

Birnie, Dunbar P. (2004): Optical video interpretation of interference colors from thin transparent films on silicon. In: *Materials Letters* 58 (22-23), S. 2795–2800. DOI: 10.1016/j.matlet.2004.04.018.

Bornemann, Nils; Dörsam, Edgar (2014): Characterization and Investigation of Large-Area, Ultra-Thin Gravure Printed Layers. Universitäts- und Landesbibliothek Darmstadt, Darmstadt.

Ebbens, Stephen; Hodgkinson, Richard; Parnell, Andrew J.; Dunbar, Alan; Martin, Simon J.; Topham, Paul D. et al. (2011): In situ imaging and height reconstruction of phase separation processes in polymer blends during spin coating. In: *ACS nano* 5 (6), S. 5124–5131. DOI: 10.1021/nn201210e.

Griesheimer, Stefan; Dörsam, Edgar; Roisman, Ilia; Bein, Thilo (2014): Farbspaltungsphänomene von Druckfarben an strukturierten Oberflächen am Beispiel des Flexodrucks. Universitäts- und Landesbibliothek Darmstadt, Darmstadt.

Hernandez-Sosa, Gerardo; Bornemann, Nils; Ringle, Ingo; Agari, Michaela; Dörsam, Edgar; Mechau, Norman; Lemmer, Uli (2013): Rheological and Drying Considerations for Uniformly Gravure-Printed Layers. Towards Large-Area Flexible Organic Light-Emitting Diodes. In: Adv. Funct. Mater. 23 (25), S. 3164–3171. DOI: 10.1002/adfm.201202862.

Kitagawa, Katsuichi (2013): Thin-film thickness profile measurement by three-wavelength interference color analysis. In: *Applied optics* 52 (10), S. 1998–2007. DOI: 10.1364/AO.52.001998.

Parthasarathy, S.; Wolf, D.; Hu, E.; Hackwood, S.; Beni, G. (1987): A color vision system for film thickness determination. In: Proceedings. 1987 IEEE International Conference on Robotics and Automation. 1987 IEEE International Conference on Robotics and Automation. Raleigh, NC, USA, March 1987: Institute of Electrical and Electronics Engineers, S. 515–519.

Raupp, Sebastian; Daume, Dominik; Tekoglu, Serpil; Merklein, Lisa; Lemmer, Uli; Hernandez-Sosa, Gerardo et al. (2017): Slot Die Coated and Flexo Printed Highly Efficient SMOLEDs. In: *Adv. Mater. Technol.* 2 (2), S. 1600230. DOI: 10.1002/admt.201600230.

Toolan, Daniel T. W. (2015): Straightforward technique for in situ imaging of spin-coated thin films. In: *Opt. Eng* 54 (2), S. 24109. DOI: 10.1117/1.OE.54.2.024109.